

# Collagen Alignment as a Predictor of Recurrence after Ductal Carcinoma *In Situ*

Matthew W. Conklin<sup>1,2</sup>, Ronald E. Gangnon<sup>2,3,4</sup>, Brian L. Sprague<sup>5</sup>, Lisa Van Gemert<sup>6</sup>, John M. Hampton<sup>2,3</sup>, Kevin W. Eliceiri<sup>2,7</sup>, Jeremy S. Bredfeldt<sup>7</sup>, Yuming Liu<sup>7</sup>, Nuntida Surachaicharn<sup>1</sup>, Polly A. Newcomb<sup>8</sup>, Andreas Friedl<sup>2,6</sup>, Patricia J. Keely<sup>†</sup>, and Amy Trentham-Dietz<sup>2,3</sup>



## Abstract

**Background:** Collagen fibers surrounding breast ducts may influence breast cancer progression. Syndecan-1 interacts with constituents in the extracellular matrix, including collagen fibers, and may contribute to cancer cell migration. Thus, the orientation of collagen fibers surrounding ductal carcinoma *in situ* (DCIS) lesions and stromal syndecan-1 expression may predict recurrence.

**Methods:** We evaluated collagen fiber alignment and syndecan-1 expression in 227 women diagnosed with DCIS in 1995 to 2006 followed through 2014 (median, 14.5 years; range, 0.7–17.6). Stromal collagen alignment was evaluated from diagnostic tissue slides using second harmonic generation microscopy and fiber analysis software. Univariate analysis was conducted using  $\chi^2$  tests and ANOVA. The association between collagen alignment z-scores, syndecan-1 staining intensity, and time to recurrence was evaluated using HRs and 95% confidence intervals (CIs).

**Results:** Greater fiber angles surrounding DCIS lesions, but not syndecan-1 staining intensity, were related to positive HER2 ( $P = 0.002$ ) status, comedo necrosis ( $P = 0.03$ ), and negative estrogen receptor ( $P = 0.002$ ) and progesterone receptor ( $P = 0.02$ ) status. Fiber angle distributions surrounding lesions included more angles closer to 90 degrees than normal ducts ( $P = 0.06$ ). Collagen alignment z-scores for DCIS lesions were positively related to recurrence (HR = 1.25; 95% CI, 0.84–1.87 for an interquartile range increase in average fiber angles).

**Conclusions:** Although collagen alignment and stromal syndecan-1 expression did not predict recurrence, collagen fibers perpendicular to the duct perimeter were more frequent in DCIS lesions with features typical of poor prognosis.

**Impact:** Follow-up studies are warranted to examine whether additional features of the collagen matrix may more strongly predict patient outcomes. *Cancer Epidemiol Biomarkers Prev*; 27(2): 138–45. ©2017 AACR.

## Introduction

Ductal carcinoma *in situ* (DCIS) is the earliest established form of breast cancer, in which the malignant cells are confined within the basement membrane of the breast ductal system. Although DCIS was a rare diagnosis prior to 1980, it now constitutes approximately 20% of all breast cancers (1); this

percentage is even higher (over 27%) in women who actively participate in mammography screening (2). It has been estimated that approximately one million women were living with a DCIS diagnosis in the United States in 2016 (3). Women with DCIS have a 4-fold elevated risk of developing an invasive breast cancer compared with the general population (4). However, many DCIS cases will not progress, and relative survival following a DCIS diagnosis approaches 100% (5). Evidence for overdiagnosis and overtreatment comes from a number of sources (6–14), indicating that surgical and radiation treatment may be unnecessary for many women with DCIS, potentially in the context of observation and endocrine risk-reducing therapy (15). Prognostic biomarkers for DCIS are needed to reduce the number of women who receive unnecessary treatment for indolent disease.

Multiple facets of the tumor microenvironment govern disease progression, including the presence of specific cell types such as macrophages, fibroblasts, or neutrophils that transition into cancer-associated variants (16–18). Changes in extracellular matrix composition (19) may potentially alter the stiffness properties of the collagen fiber matrix (20), which is linked to increased tumor formation and changes in gene/protein expression (21). However, the influence of the collagen matrix manifests in functional ways as well. In a mouse mammary tumor model, changes in the orientation of collagen fibers with respect to the tumor/stroma boundary have been observed and termed tumor-associated collagen signatures (TACS; ref. 22). This observation has been

<sup>1</sup>Department of Cell and Regenerative Biology, University of Wisconsin-Madison, Madison, Wisconsin. <sup>2</sup>Carbone Cancer Center, School of Medicine and Public Health, University of Wisconsin-Madison, Madison, Wisconsin. <sup>3</sup>Department of Population Health Sciences, University of Wisconsin-Madison, Madison, Wisconsin. <sup>4</sup>Department of Biostatistics and Medical Informatics, University of Wisconsin-Madison, Madison, Wisconsin. <sup>5</sup>Department of Surgery, University of Vermont, Burlington, Vermont. <sup>6</sup>Department of Pathology and Laboratory Medicine, University of Wisconsin-Madison, Madison, Wisconsin. <sup>7</sup>Laboratory for Optical and Computational Instrumentation, University of Wisconsin-Madison, Madison, Wisconsin. <sup>8</sup>Fred Hutchinson Cancer Research Center, Seattle, Washington.

**Note:** Supplementary data for this article are available at Cancer Epidemiology, Biomarkers & Prevention Online (<http://cebp.aacrjournals.org/>).

<sup>†</sup>Deceased.

**Corresponding Author:** Amy Trentham-Dietz, University of Wisconsin-Madison, 610 Walnut St., WARF Room 307, Madison WI, 53726. Phone: 608-265-4175; Fax: 608-265-5330; E-mail: [trentham@wisc.edu](mailto:trentham@wisc.edu)

doi: 10.1158/1055-9965.EPI-17-0720

©2017 American Association for Cancer Research.

extended to a cohort of women with invasive ductal carcinoma where the observation of collagen fibers oriented perpendicularly to tumor cells predicted decreased survival (23). This result raises the question whether collagen fiber orientation is altered at earlier disease stages.

We have also examined the role of cell signaling pathways in progression including effects of the heparan sulfate proteoglycan, syndecan-1, in loss of growth control in cancer and its effects on the extracellular matrix. Expression of syndecan-1 by stromal fibroblasts in the tumor microenvironment engages a reciprocal, carcinoma growth-promoting feedback loop (24). In xenograft experiments, the presence of fibroblasts expressing syndecan-1 resulted in an 88% increase in tumor growth compared with mixed suspensions with syndecan-1-deficient fibroblasts (25); elevated microvessel density (by 36%) and vessel area (by 153%) were also observed. This finding was validated in 207 invasive breast cancer patient samples, where stromal syndecan-1 expression was associated with increased vessel density and higher average vessel area (25) as well as the TACS signature (23). These results support the hypothesis that expression of syndecan-1 in carcinoma-associated fibroblasts stimulates changes in collagen architecture associated with tumor progression. Furthermore, forced syndecan-1 expression in mammary fibroblasts leads to the production of an extracellular matrix with aligned fibers *in vitro*, so that the extracellular matrix is permissive to the directional migration and invasion of breast carcinoma cells (26).

On the basis of these promising results in experimental models and invasive breast cancer tumors, we examined whether the realignment of the extracellular matrix plays a role in recurrence after DCIS. We also evaluated whether the presence of syndecan-1 expression in stromal fibroblasts was associated with collagen alignment and recurrence. In addition, we compared collagen alignment and stromal syndecan-1 expression in ducts containing DCIS to normal ducts, and characterized clinical and histopathologic features of DCIS lesions according to collagen alignment and syndecan-1 expression. Thus, the purpose of this analysis was to evaluate whether collagen alignment around DCIS lesions was associated with recurrence after consideration of important histopathologic and patient factors.

## Materials and Methods

### Study population

We evaluated the tumor microenvironment in relation to disease-free survival after a DCIS diagnosis using data from the Wisconsin In Situ Cohort (WISC). This study was approved by

the University of Wisconsin Health Sciences Human Subjects Committee. WISC consists of 2,238 women diagnosed with breast carcinoma *in situ* (1,930 with DCIS) in Wisconsin during 1995 to 2006. Characteristics of the study population have been published (27–29). All participants were female residents of Wisconsin with a first primary diagnosis of breast carcinoma *in situ* reported to Wisconsin's mandatory tumor registry during 1995 to 2006 and capable of granting a telephone interview. Eligibility was limited to cases aged <75 years (median 55.9) with known dates of diagnosis and listed telephone numbers. Overall, 78% of eligible cases enrolled at baseline, providing verbal informed consent. The Wisconsin tumor registry provided data regarding the DCIS diagnosis, including patient age, date of diagnosis, tumor histology, grade, and treatment. Follow-up interviews with cohort subjects were conducted at 2-year intervals through 2014 to update health information, including treatment history and any new breast cancer diagnoses (including recurrences and second primary events). For women that reported a new breast diagnosis, pathology reports were obtained to validate these diagnoses using informed consent forms signed by the participants.

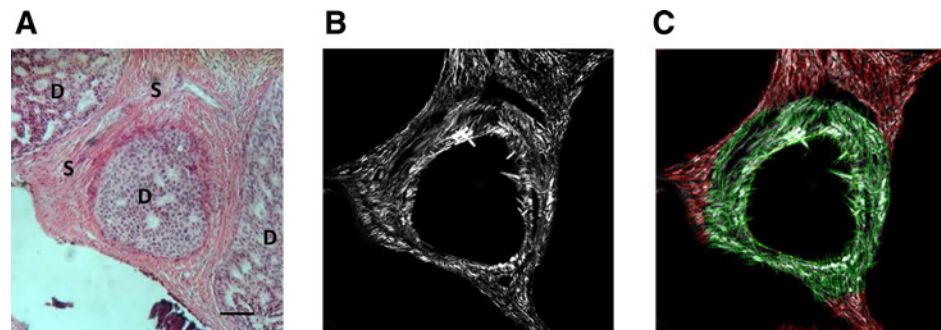
At the end of the baseline interview, a sequential subset of subjects was asked to provide written informed consent to access their medical records and tumor blocks for pathology review and IHC analysis. Of 640 women invited to this substudy, 382 (60%) women agreed to participate. Complete pathology and tumor block samples were available for 336 women (90%). All tumor block samples were visually scored for ER, PR, and HER2/neu staining using standard antibodies (30).

### SHG imaging microscopy

Second harmonic generation (SHG) on a multiphoton microscope was used to image collagen fibers as described previously (Fig. 1; Supplementary Fig. S1; ref. 31). The excitation used 890 nm, 100 fs pulses from a commercial Ti:Sapphire oscillator (Mira, Coherent). The multiphoton scanning microscope was a modified Fluoview300 (Olympus) mounted on a fixed stage upright stand (Olympus BX61). All imaging was performed with a 10× (0.5 N.A) air objective lens. To excite all orientations equally, circularly polarized light was used throughout. This was achieved at the focal plane using the combination of a quarter wave plate and a half wave plate as a compensator (31). The SHG was collected in the forward direction by a 0.9 N.A condenser, isolated with a 20 nm bandwidth 445 nm bandpass filter (Semrock) and detected by a single photon counting photomultiplier tube module (Hamamatsu 7421). Images were acquired at two times zoom

**Figure 1.**

Process for evaluating collagen fiber alignment around DCIS lesions. **A**, Routine H&E slides from the tissue blocks at the baseline diagnosis. Scale bar, 100  $\mu$ m. D, DCIS lesion; S, stroma. **B**, SHG microscopy generated a high-contrast image of the lesion composed solely of collagen. **C**, The SHG image was transformed using the curvelet algorithm and the angle of curvelets with respect to the DCIS foci boundary within a 100- $\mu$ m radius (green) was calculated using customized software. Images are 750  $\mu$ m<sup>2</sup>.



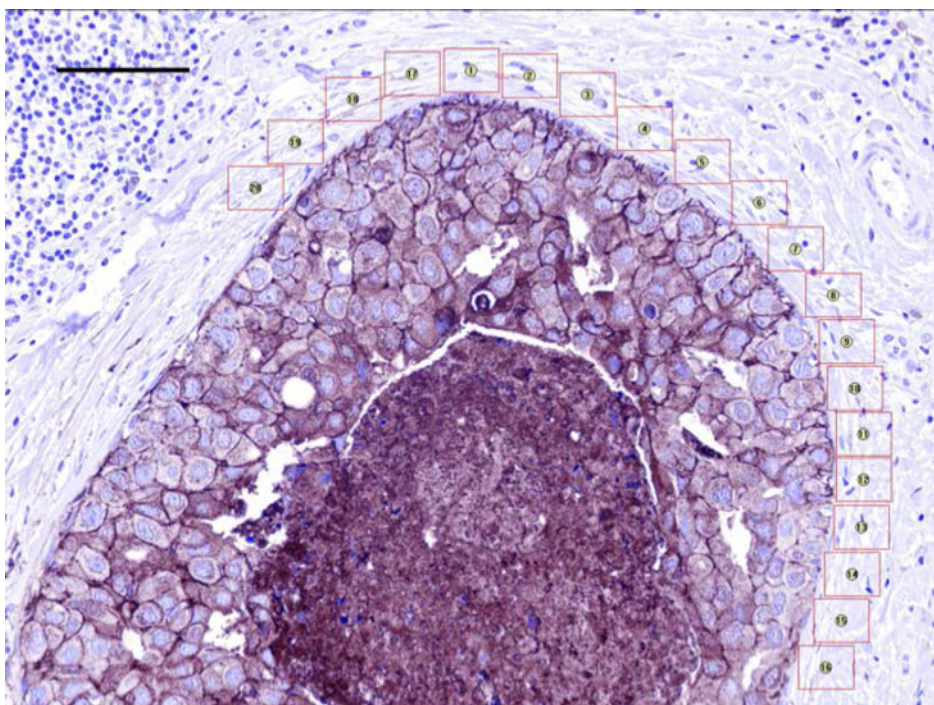


**Figure 2.** DCIS lesion with staining for syndecan-1 in the stromal fibroblasts. Rectangular boxes placed around the lesion boundary were evaluated for staining intensity. Scale bar, 100  $\mu\text{m}$ .

with a field-of-view of approximately  $750 \mu\text{m}^2$  and a resolution of  $1,024 \times 1,024$  pixels. On each tissue slide, SHG images were acquired for an average of 4.6 (range, 2–7) DCIS lesions (one slide/woman) or normal ducts (one additional slide/woman, when available).

Each DCIS slide was rated by a trained reviewer (M.W. Conklin) for the presence of TACS, while blinded to outcome using established definitions of collagen organization (22, 23). Briefly, TACS (previously labeled TACS-3 in ref. 23 but referred to simply as TACS herein) collagen fiber organization is typified by orientation in a perpendicular pattern with respect to the tumor/stroma boundary. Collagen alignment was also evaluated in normal ducts for a subset of DCIS patients ( $N = 100$  patients; mean number of ducts 4.5, range 2–5). All imaging locations were also photographed using a digital camera mounted to the eyepiece for the purpose of pathology verification and examination.

#### Computer-based quantitation of collagen features

A custom-written open-source software package (CurveAlign) was used to analyze SHG images, which is available for free download at (<http://loci.wisc.edu/software/curvealign>; refs. 32, 33). The program executes a curvelet transform of the SHG image, which is a multiscale, orientation-sensitive version of the wavelet transform where edges in image features are identified. Each curvelet has an  $x$ - $y$  location in the image, as well as an orientation. Individual curvelets are small; thus, several may be assigned to a single collagen fiber. A boundary separating the collagen matrix from breast epithelial cells was manually drawn in the program. CurveAlign then measured the angle of the curvelet with respect to that boundary for each individual curvelet and tabulated the results into a histogram and summary statistics (mean, mode, etc.). We also instructed the software to restrict the analysis to only those curvelets within a 100- $\mu\text{m}$  radius from the drawn boundary. This was done to lessen the contribution of distant collagen and

fibers that are associated with neighboring foci or blood vessels. Hundreds of curvelets were measured per patient.

#### Syndecan-1 expression

Syndecan-1 expression was evaluated in the tumor samples by chromogenic IHC using a mouse mAb to syndecan-1 (clone B-B4, Serotec) on a Ventana automated instrument, as described previously (34). Negative control slides consistently yielded an undetectable staining signal. Multiple lesions were evaluated on each tissue slide (mean, 2.7; range, 1–5). Expression of syndecan-1 was evaluated in the stromal fibroblasts by placing an average of 21 (range, 10–45) rectangular boxes (regions of interest) of equal size (40 by 32  $\mu\text{m}$ ) on the area surrounding ducts on digital images of the tissue slides (Fig. 2; Supplementary Fig. S2). All slides were evaluated for staining intensity blinded to outcome using Vectra automated imaging with inForm Cell Analysis software (PerkinElmer) that produced a staining signal averaged over the areas in the rectangular boxes.

#### Statistical analyses

Collagen fiber angles for normal ducts and DCIS lesions were classified as the percent of fibers relative to the lesion boundary distributed across 5-degree angle bins (1–5, 6–10, 11–15, . . . , 86–90 degrees). A probit (latent normal) model for ordinal compositional data was used to create a unidimensional collagen alignment score (latent  $z$ -score) for the distribution of fiber angles in a single DCIS lesion or normal duct using the ordinal package in R (35). Larger collagen alignment scores indicate a greater proportion of fibers angled perpendicularly relative to the duct, whereas smaller collagen alignment scores represent fibers with orientations more parallel to the duct. Collagen alignment scores and staining signals of syndecan-1 were averaged to summarize the multiple measurements for each subject and tissue type. Missing data were imputed using the `aregImpute` function in the `Hmisc`

package in R (36, 37). Pearson correlation coefficients were calculated to describe the associations between average syndecan-1 staining intensity and the collagen alignment score in normal ducts and lesions.

The primary outcome was time to first recurrence. Kaplan-Meier curves were calculated for subjects with high (above the median) and low (below the median) scores for collagen alignment and syndecan-1 staining intensity; curves with 95% confidence bands are presented for the first imputed dataset for collagen alignment score. Cox proportional hazards models were used to estimate univariate HRs and 95% confidence intervals (CI) of recurrence for an interquartile range (IQR) increase in collagen alignment and syndecan-1 staining intensity scores. The univariate HR and 95% CI of recurrence associated with the TACS pattern were also estimated.

Using the tumor slides obtained at baseline, we analyzed collagen alignment score and staining signal of syndecan-1 in the stromal tissue surrounding DCIS lesions for 230 women. Among the DCIS cases, collagen alignment was available for 227 DCIS patients and 100 patients with adjacent normal ducts, and syndecan-1 staining was available for 125 DCIS lesions.

## Results

DCIS cases were followed for a median of 14.5 years (range, 0.7–17.6). Among the 227 cases, 36 (16%) experienced a recurrence including 18 DCIS and 16 invasive breast cancer diagnoses; 18 cases experienced ipsilateral recurrences (10 DCIS, 8 invasive), while 16 cases had contralateral recurrences (8 DCIS, 8 invasive). Both cases with recurrences of unknown stage occurred in ipsilateral breasts.

The first quartile, median, and third quartile of the collagen alignment scores for DCIS lesions were  $-0.085$ ,  $0.014$ , and  $0.159$ , respectively, which correspond to 14.7%, 17.2%, and 21.1% of fiber angles greater than 45 degrees relative to the duct; the minimum and maximum collagen alignment scores for DCIS lesions were  $-0.708$  (4.7%) and  $0.553$  (34.1%). A greater proportion of collagen fibers surrounding DCIS lesions were angled relatively perpendicular to the ductal boundary, more angles closer to 90 degrees, than those surrounding normal ducts ( $P = 0.058$  by paired  $t$  test; Fig. 3).

When visually assessed by a trained reviewer, 50% of the DCIS cases lacked the TACS pattern of collagen alignment in their tumor samples regardless of the number of lesions evaluated (range, 2–5). The TACS pattern was observed in all lesions evaluated for only 2 (1%) cases, whereas some but not all of the lesions evaluated for the remaining 49% of cases exhibited the TACS pattern. The TACS pattern of collagen fibers was observed more frequently among DCIS lesions that exhibited comedo necrosis and were estrogen receptor (ER) negative, progesterone receptor (PR) negative, and HER2 positive (Table 1). Presence of the TACS pattern was not strongly associated with age, tumor grade, multifocal lesions, or treatment. Furthermore, the TACS pattern was not associated with recurrence (HR = 1.51; 95% CI, 0.77–2.95).

The quantified collagen alignment scores surrounding DCIS lesions and adjacent normal ducts were not strongly correlated ( $r = -0.06$ ,  $P = 0.77$ ). Collagen alignment scores for DCIS lesions were positively, but not significantly, related to recurrence (HR = 1.25; 95% CI, 0.84–1.87 for an IQR increase in average fiber angles; Fig. 4); collagen alignment scores for normal ducts

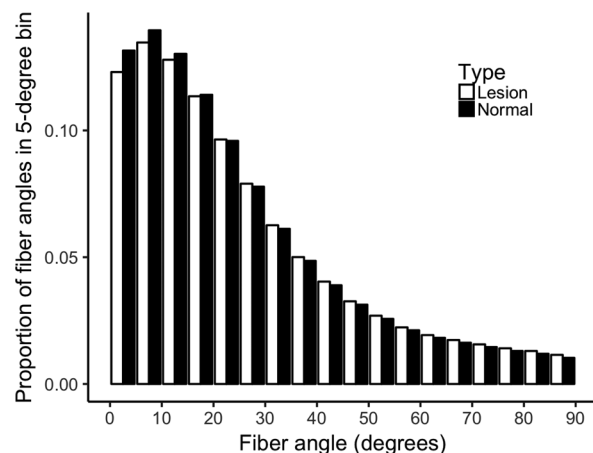


**Figure 3.**

Proportion of collagen fiber angles in 5 degree bins relative to the ductal boundary for median collagen alignment score in normal ducts (white) and DCIS lesions (black).

were not related to recurrence (HR = 0.86; 95% CI, 0.57–1.29 per IQR increase).

Syndecan-1 staining intensity was not associated with patient, tumor, or treatment characteristics in this cohort of DCIS cases (Table 1), although there was a suggestion that staining intensity was stronger in women with ER-negative lesions ( $P = 0.07$ ). Average syndecan-1 staining intensity was not related to recurrence (HR = 0.92; 95% CI, 0.69–1.22 for an IQR increase in staining intensity; Fig. 5). Syndecan-1 staining intensity was also not correlated with collagen fiber alignment around DCIS lesions ( $r = 0.08$ ,  $P = 0.51$ ) or normal ducts ( $r = 0.09$ ,  $P = 0.65$ ).

## Discussion

Motivated by prior studies of invasive breast cancer, we examined whether collagen alignment surrounding DCIS lesions was associated with recurrence. Quantitative collagen alignment measurement using novel analysis of SHG microscopy images detected a very modest trend for lesions, measured at the time of diagnosis, to have more collagen fibers oriented closer to 90 degrees than normal ducts. Collagen alignment scores did not predict recurrence. However, we did observe that the TACS pattern was more common in DCIS lesions with markers of poor prognosis, including ER, PR, and HER2 status as well as comedo necrosis. Although TACS is evaluated subjectively, this confirms our prior study in invasive breast cancer (23) and suggests that features of the collagen fiber matrix beyond orientation, such as fiber straightness and density, may predict malignant potential.

The role of DCIS in the natural history of many breast cancer tumors is uncertain. Regardless of treatment received, relative survival following a DCIS diagnosis approaches 100% despite the 4-fold elevated risk of developing an invasive breast cancer compared with the general population (5). Thus, DCIS is considered a nonobligate precursor and many DCIS patients will not develop invasive breast cancer; at the same time, it is uncertain whether all invasive breast cancers first grow through an *in situ* stage (DCIS or other type of *in situ*) or progress directly to invasive disease (4). Relatively few histopathologic or biological markers

**Table 1.** Characteristics of DCIS cases according to collagen alignment and syndecan-1 staining around DCIS lesions, WISC study

Characteristics <sup>a</sup>	Collagen alignment (n = 227)			Syndecan-1 staining (n = 125)		P <sup>c</sup>
	Total no.	TACS (%)	P <sup>b</sup>	Total no.	Average staining signal	
Age						
20-49	72	44.4		39	0.0129	
50-64	105	50.5		54	0.0158	
65-74	50	56.0	0.45	32	0.0139	0.58
Tumor grade						
Low	46	46.7		24	0.0148	
Intermediate	88	51.7		45	0.0145	
High	93	49.6	0.71	56	0.0140	0.57
Comedo necrosis						
Absent	105	41.9		53	0.0128	
Present	122	56.6	0.03	72	0.0155	0.24
Multifocality						
Absent	73	51.2		44	0.0132	
Present	154	49.1	0.74	81	0.0150	0.32
Method of detection						
Symptomatic	35	63.0		21	0.0187	
Mammography	192	47.4	0.09	104	0.0135	0.34
ER status						
Negative	35	74.3		22	0.0227	
Positive	192	45.3	0.002	103	0.0126	0.07
PR status						
Negative	77	60.7		39	0.0173	
Positive	150	44.2	0.02	86	0.0131	0.22
HER2 status						
Negative	102	45.3		45	0.0119	
Equivocal	63	38.8		42	0.0131	
Positive	62	68.2	0.002	38	0.0187	0.18
Treatment						
BCS	42	55.3		19	0.0127	
BCS with radiation	98	43.9		55	0.0142	
Mastectomy	87	53.7	0.28	51	0.0153	0.54
Endocrine therapy						
No	164	51.6		87	0.0141	
Yes	63	45.2	0.43	38	0.0150	0.56

Abbreviations: BCS, breast conserving surgery; TACS, tumor-associated collagen signature.

<sup>a</sup>At baseline. Missing data were imputed for grade (n = 141), multifocality (n = 20), method of detection (n = 1), ER status (n = 1), PR status (n = 3), HER2 status (n = 5), surgical treatment (n = 66), and endocrine therapy (n = 60). Zero cases were missing data for age or comedo necrosis.

<sup>b</sup>From  $\chi^2$  tests of the association between patient characteristics and TACS present in at least one DCIS duct.

<sup>c</sup>From two-sided t tests using ANOVA.

have been established as predictive of recurrence or invasion after DCIS. Comedo type architecture, high-grade, and larger tumor size are associated with small (~2-fold) increases in the likelihood of recurrence after DCIS (38–41). Although expression of HER2/neu, p53, ER, and PR do not appear to be strong independent predictors of recurrence after a DCIS diagnosis (42, 43), the Oncotype DX DCIS score has shown promise for predicting local recurrence and guiding treatment decision making for certain low-risk DCIS cases based on lesion size, grade, and surgical margin (44–46). We did not have available data for the Oncotype DX DCIS score to compare to the collagen alignment score, although our study did suggest that TACS is correlated with comedo necrosis, ER and PR negativity, and HER2 positivity. PR is one of 7 cancer-related genes included in the Oncotype DX DCIS score.

Although most research has thus focused on characterizing the cancerous DCIS cells, laboratory studies have recently demonstrated the important role of the tumor microenvironment in breast cancer progression. Aside from malignant epithelial cells, the tumor microenvironment consists of several types of nonneoplastic stromal cells and an extracellular matrix of collagen, proteoglycans, and other molecules. Sev-

eral lines of evidence suggest that breast tumorigenesis is critically influenced by active signaling between malignant breast epithelial cells and the nonneoplastic cells of the tumor microenvironment (47). A number of investigators have used *in vitro*- and *in vivo*-based assays to demonstrate that experimental manipulation of the stromal microenvironment can profoundly affect tumor cell growth, invasion, and metastasis (48). Thus, alterations in the tumor environment, rather than the neoplastic cells themselves, may dictate the DCIS-to-invasive stage transition.

We have shown previously that the orientation of collagen fibers may lead to enhanced directional persistence of breast cells with malignant potential (20). Using tumor explants in three-dimensional culture, we showed that local cell invasion was found predominantly along radially aligned collagen fibers (22). Others have also found that breast cancer cells in a collagen composite extracellular matrix appear to follow collagen fiber alignment direction during intravasation (49). Syndecan-1 expression in breast carcinoma stromal fibroblasts may promote the realignment of the extracellular matrix into parallel arrangements that is permissive to breast carcinoma directional migration and invasion (26). This study did not extend these findings

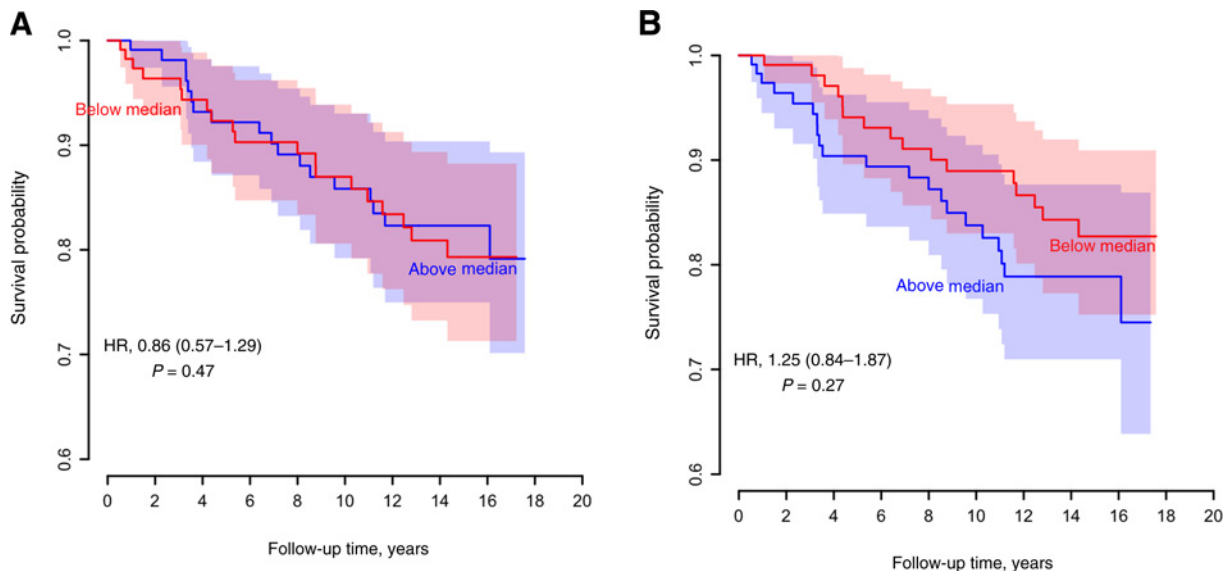


**Figure 4.**

Kaplan-Meier estimates for time to recurrence as a function of collagen alignment score (above and below the median) from the first imputed dataset for normal ducts (A) and DCIS lesions (B). Univariate HR for IQR increase in collagen alignment score from Cox proportional hazards regression with collagen alignment score as a continuous (linear) predictor. Shaded regions reflect 95% confidence bands for the survival curves.

regarding syndecan-1 expression in the setting of invasive breast cancer to the archived tumor samples from our DCIS cohort. Evaluation of syndecan-1 was limited as 45% of the cases had tumor tissue slides that were inadequate for syndecan-1 assessment; the small sample size reduced statistical power to detect modest associations. Ongoing research concerning breast cancer progression will need to consider both biological factors, including those associated with the tumor microenvironment as well as

nonbiological features such as quality of imaging, technical skills of specialty providers, and adherence to recommendations for the standard of care.

Although the size of the DCIS cohort limited identification of associations between the collagen alignment score, syndecan-1 staining intensity, and disease-free survival, other features of our study bear consideration. This is the first study to evaluate collagen alignment in the DCIS setting. TACS was assessed without knowledge of recurrence outcomes; concordance in TACS assessment between the baseline diagnosis and recurrence was not evaluated, although this would be an important area for future studies where tissue samples are available for both diagnoses. Notably, our approach for evaluating collagen fiber orientation relative to the tumor-stroma boundary using SHG microscopy is unique. Other groups have used similar microscopy with differing algorithms for evaluating collagen fiber alignment in invasive breast cancer (50–52), ovarian cancer (53), and engineered cardiovascular tissue (54). Furthermore, the DCIS cohort has extensive follow-up (up to 17 years after diagnosis), and our approach to the statistical analysis took full advantage of ordinal nature of the data to efficiently use the available data via dimension reduction.

In summary, these results underscore the relevance of the breast tumor microenvironment to malignant potential, in particular the arrangement of the collagen fiber matrix. The distribution of fiber angles relative to the DCIS boundary appears to be skewed toward a perpendicular orientation, whereas fibers surrounding normal ducts are more parallel to the stromal boundary. Fiber orientation patterns that are more perpendicular are also more common in DCIS lesions with features typical of poor prognosis in breast cancer. Future research is warranted to discover additional features of the collagen matrix that may more strongly predict patient outcomes.

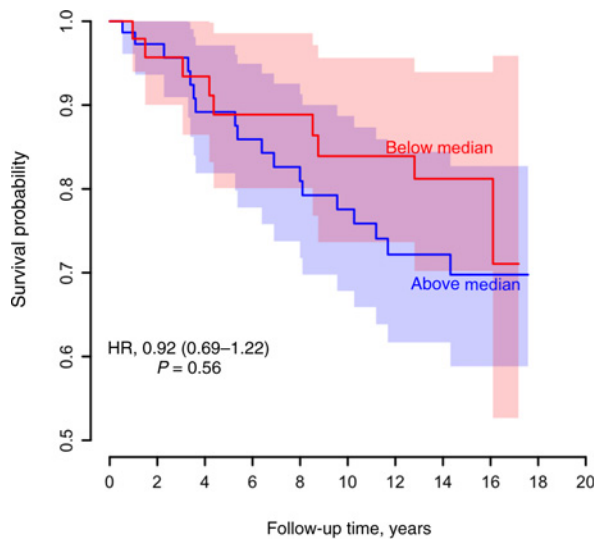


**Figure 5.**

Kaplan-Meier estimates for time to recurrence as a function of average syndecan-1 staining intensity (above and below the median). Univariate HR for IQR increase in staining intensity from Cox proportional hazards regression with average syndecan-1 staining intensity as a continuous (linear) predictor. Shaded regions reflect 95% confidence bands for the survival curves.

#### Disclosure of Potential Conflicts of Interest

No potential conflicts of interest were disclosed.

Conklin et al.

**Disclaimer**

The funding bodies have no role in the design of the study and collection, analysis, and interpretation of data and in writing the article.

**Authors' Contributions**

**Conception and design:** M.W. Conklin, B.L. Sprague, A. Friedl, P.J. Keely, A. Trentham-Dietz

**Development of methodology:** M.W. Conklin, R.E. Gangnon, J.S. Bredfeldt, A. Friedl, P.J. Keely, A. Trentham-Dietz

**Acquisition of data (provided animals, acquired and managed patients, provided facilities, etc.):** M.W. Conklin, L. van Germert, J.M. Hampton, K.W. Eliceiri, N. Surachaicharn, P.A. Newcomb, A. Trentham-Dietz, P.J. Keely  
**Analysis and interpretation of data (e.g., statistical analysis, biostatistics, computational analysis):** M.W. Conklin, R.E. Gangnon, B.L. Sprague, J.M. Hampton, K.W. Eliceiri, J.S. Bredfeldt, Y. Liu, N. Surachaicharn, A. Trentham-Dietz, P.J. Keely

**Writing, review, and/or revision of the manuscript:** M.W. Conklin, R.E. Gangnon, B.L. Sprague, J.M. Hampton, J.S. Bredfeldt, P.A. Newcomb, A. Friedl, A. Trentham-Dietz, P.J. Keely

**Administrative, technical, or material support (i.e., reporting or organizing data, constructing databases):** J.M. Hampton, A. Trentham-Dietz, P.J. Keely  
**Study supervision:** A. Trentham-Dietz, P.J. Keely

**References**

- Howlander N, Noone AM, Krapcho M, Miller D, Bishop K, Kosary CL, et al. SEER Cancer Statistics Review, 1975–2014. Bethesda, MD: NCI; 2017. Available from: [https://seer.cancer.gov/csr/1975\\_2014/](https://seer.cancer.gov/csr/1975_2014/).
- Miglioretti DL, Zhu W, Kerlikowske K, Sprague BL, Onega T, Buist DS, et al. Breast tumor prognostic characteristics and biennial vs. annual mammography, age, and menopausal status. *JAMA Oncol* 2015;1:1069–77.
- Sprague BL, Trentham-Dietz A. Prevalence of breast carcinoma *in situ* in the United States. *JAMA* 2009;302:846–8.
- Sprague BL, Trentham-Dietz A. *In situ* Breast Cancer. In: Li CI, editor. *Breast Cancer Epidemiology*. New York, NY: Springer; 2010. p. 47–72.
- Warnberg F, Yuen J, Holmberg L. Risk of subsequent invasive breast cancer after breast carcinoma *in situ*. *Lancet* 2000;355:724–5.
- Ernster VL, Barclay J. Increases in ductal carcinoma *in situ* (DCIS) of the breast in relation to mammography: a dilemma. *J Natl Cancer Inst Monogr* 1997;1:151–6.
- Duffy SW, Agbaje O, Tabar L, Vitak B, Bjurstam N, Bjorneld L, et al. Overdiagnosis and overtreatment of breast cancer: estimates of overdiagnosis from two trials of mammographic screening for breast cancer. *Breast Cancer Res* 2005;7:258–65.
- Esserman L, Shieh Y, Thompson I. Rethinking screening for breast cancer and prostate cancer. *JAMA* 2009;302:1685–92.
- Zackrisson S, Andersson I, Janzon L, Manjer J, Garne JP. Rate of overdiagnosis of breast cancer 15 years after end of Malmo mammographic screening trial: follow-up study. *BMJ* 2006;332:689–92.
- Betsill WL Jr, Rosen PP, Lieberman PH, Robbins GF. Intraductal carcinoma. Long-term follow-up after treatment by biopsy alone. *JAMA* 1978;239:1863–7.
- Rosen PP, Braun DW Jr, Kinne DE. The clinical significance of pre-invasive breast carcinoma. *Cancer* 1980;46:919–25.
- Page DL, Dupont WD, Rogers LW, Landenberger M. Intraductal carcinoma of the breast: follow-up after biopsy only. *Cancer* 1982;49:751–8.
- Eusebi V, Feudale E, Foschini MP, Micheli A, Conti A, Riva C, et al. Long-term follow-up of *in situ* carcinoma of the breast. *Semin Diagn Pathol* 1994;11:223–35.
- Welch HG, Black WC. Using autopsy series to estimate the disease "reservoir" for ductal carcinoma *in situ* of the breast: how much more breast cancer can we find? *Ann Intern Med* 1997;127:1023–8.
- Esserman L, Yau C. Rethinking the standard for ductal carcinoma *in situ* treatment. *JAMA Oncol* 2015;1:881–3.
- Garcia-Mendoza MG, Inman DR, Ponik SM, Jeffery JJ, Sheerar DS, Van Doorn RR, et al. Neutrophils drive accelerated tumor progression in the collagen-dense mammary tumor microenvironment. *Breast Cancer Res* 2016;18:49.
- Lewis CE, Pollard JW. Distinct role of macrophages in different tumor microenvironments. *Cancer Res* 2006;66:605–12.
- Cirri P, Chiarugi P. Cancer associated fibroblasts: the dark side of the coin. *Am J Cancer Res* 2011;1:482–97.
- Naba A, Clauser KR, Hoersch S, Liu H, Carr SA, Hynes RO. The matrisome: in silico definition and in vivo characterization by proteomics of normal and tumor extracellular matrices. *Mol Cell Proteomics* 2012;11:M111014647.
- Riching KM, Cox BL, Salick MR, Pehlke C, Riching AS, Ponik SM, et al. 3D collagen alignment limits protrusions to enhance breast cancer cell persistence. *Biophys J* 2014;107:2546–58.
- Finak G, Bertos N, Pepin F, Sadekova S, Souleimanova M, Zhao H, et al. Stromal gene expression predicts clinical outcome in breast cancer. *Nat Med* 2008;14:518–27.
- Provenzano PP, Eliceiri KW, Campbell JM, Inman DR, White JC, Keely PJ. Collagen reorganization at the tumor-stromal interface facilitates local invasion. *BMC Med* 2006;4:38.
- Conklin MW, Eickhoff JC, Riching KM, Pehlke CA, Eliceiri KW, Provenzano PP, et al. Aligned collagen is a prognostic signature for survival in human breast carcinoma. *Am J Pathol* 2011;178:1221–32.
- Maeda T, Alexander CM, Friedl A. Induction of syndecan-1 expression in stromal fibroblasts promotes proliferation of human breast cancer cells. *Cancer Res* 2004;64:612–21.
- Maeda T, Desouky J, Friedl A. Syndecan-1 expression by stromal fibroblasts promotes breast carcinoma growth in vivo and stimulates tumor angiogenesis. *Oncogene* 2006;25:1408–12.
- Yang N, Mosher R, Seo S, Beebe D, Friedl A. Syndecan-1 in breast cancer stroma fibroblasts regulates extracellular matrix fiber organization and carcinoma cell motility. *Am J Pathol* 2011;178:325–35.
- Sprague BL, McLaughlin V, Hampton JM, Newcomb PA, Trentham-Dietz A. Disease-free survival by treatment after a DCIS diagnosis in a population-based cohort study. *Breast Cancer Res Treat* 2013;141:145–54.
- McLaughlin VH, Trentham-Dietz A, Hampton JM, Newcomb PA, Sprague BL. Lifestyle factors and the risk of a second breast cancer after ductal carcinoma *in situ*. *Cancer Epidemiol Biomarkers Prev* 2014;23:450–60.
- Sprague BL, Trentham-Dietz A, Nichols HB, Hampton JM, Newcomb PA. Change in lifestyle behaviors and medication use after a diagnosis of ductal carcinoma *in situ*. *Breast Cancer Res Treat* 2010;124:487–95.
- Walsh M, Trentham-Dietz A, Newcomb P. Characteristics of comedo type ductal carcinoma *in situ* (DCIS) of the breast in relation to reproductive factors and molecular markers. *Am J Epidemiol* 2007;165(Suppl):S33.

**Acknowledgments**

This work was supported in part by the NCI (grant numbers P30 CA014520, R01 CA067264, R01 CA199996, and U54 CA163303), the Congressionally Directed Medical Research Program (grant number W81XWH-11-1-0214), and the University of Wisconsin Institute for Clinical and Translational Research, which is supported by the NIH (grant number UL1 TR000427).

The authors thank Julie McGregor, Kathy Peck, Karen Johnson, Hazel Nichols, and Paul Campagnola for their assistance with data collection. We also wish to thank Laura Stephenson and the Wisconsin Cancer Reporting System for support in providing cancer registry data. The authors also thank the University of Wisconsin Translational Research Initiatives in Pathology Laboratory, in part supported by the UW Department of Pathology and Laboratory Medicine and UWCCC grant CA014520 for use of its facilities and services.

The costs of publication of this article were defrayed in part by the payment of page charges. This article must therefore be hereby marked *advertisement* in accordance with 18 U.S.C. Section 1734 solely to indicate this fact.

Received August 3, 2017; revised September 26, 2017; accepted November 1, 2017; published OnlineFirst November 15, 2017.

31. Chen X, Nadiarynkh O, Plotnikov S, Campagnola PJ. Second harmonic generation microscopy for quantitative analysis of collagen fibrillar structure. *Nat Protoc* 2012;7:654–69.
32. Bredfeldt JS, Liu Y, Conklin MW, Keely PJ, Mackie TR, Eliceiri KW. Automated quantification of aligned collagen for human breast carcinoma prognosis. *J Pathol Inform* 2014;5:28.
33. Liu Y, Keikhosravi A, Mehta GS, Drifka CR, Eliceiri KW. Methods for quantifying fibrillar collagen alignment. In: Rittie L, editor. *Fibrosis: Methods and Protocols*. New York, NY: Humana Press; 2017.
34. Baba F, Swartz K, van Buren R, Eickhoff J, Zhang Y, Wolberg W, et al. Syndecan-1 and syndecan-4 are overexpressed in an estrogen receptor-negative, highly proliferative breast carcinoma subtype. *Breast Cancer Res Treat* 2006;98:91–8.
35. Christensen RHB. Regression models for ordinal data. R package version 2015.6–28. Vienna, Austria: R Foundation for Statistical Computing; 2015. Available from: <https://cran.r-project.org/web/packages/ordinal/>.
36. Harrell FE Jr. Hmisc: Harrell Miscellaneous. R package version 3.17–4. Vienna, Austria: R Foundation for Statistical Computing; 2016. Available from: <https://cran.r-project.org/web/packages/Hmisc/>.
37. R Core Team. R: A language and environment for statistical computing. Vienna, Austria: R Foundation for Statistical Computing; 2016. Available from: <http://www.R-project.org/>.
38. Boyages J, Delaney G, Taylor R. Predictors of local recurrence after treatment of ductal carcinoma *in situ*: a meta-analysis. *Cancer* 1999;85:616–28.
39. Habel LA, Daling JR, Newcomb PA, Self SC, Porter PL, Stanford JL, et al. Risk of recurrence after ductal carcinoma *in situ* of the breast. *Cancer Epidemiol Biomarkers Prev* 1998;7:689–96.
40. Kerlikowske K, Molinaro A, Cha I, Ljung BM, Ernster VL, Stewart K, et al. Characteristics associated with recurrence among women with ductal carcinoma *in situ* treated by lumpectomy. *J Natl Cancer Inst* 2003;95:1692–702.
41. Li CL, Malone KE, Saltzman BS, Daling JR. Risk of invasive breast carcinoma among women diagnosed with ductal carcinoma *in situ* and lobular carcinoma *in situ*, 1988–2001. *Cancer* 2006;106:2104–12.
42. Barnes NL, Khavari S, Boland GP, Cramer A, Knox WF, Bundred NJ. Absence of HER4 expression predicts recurrence of ductal carcinoma *in situ* of the breast. *Clin Cancer Res* 2005;11:2163–8.
43. Cornfield DB, Palazzo JP, Schwartz GF, Goonewardene SA, Kovatich AJ, Chervoneva I, et al. The prognostic significance of multiple morphologic features and biologic markers in ductal carcinoma *in situ* of the breast: a study of a large cohort of patients treated with surgery alone. *Cancer* 2004;100:2317–27.
44. Rakovitch E, Nofech-Mozes S, Hanna W, Baehner FL, Saskin R, Butler SM, et al. A population-based validation study of the DCIS Score predicting recurrence risk in individuals treated by breast-conserving surgery alone. *Breast Cancer Res Treat* 2015;152:389–98.
45. Sgroi DC, Nofech-Mozes S, Hanna W, Sutradhar R, Baehner FL, Miller DP, et al. Multigene expression assay and benefit of radiotherapy after breast conservation in ductal carcinoma *in situ*. *J Natl Cancer Inst* 2017;109:djw256.
46. Solin LJ, Gray R, Baehner FL, Butler SM, Hughes LL, Yoshizawa C, et al. A multigene expression assay to predict local recurrence risk for ductal carcinoma *in situ* of the breast. *J Natl Cancer Inst* 2013;105:701–10.
47. Sgroi DC. Preinvasive breast cancer. *Annu Rev Pathol* 2010;5:193–221.
48. Grum-Schwensen B, Klingelhofer J, Berg CH, El-Naaman C, Grigorian M, Lukanidin E, et al. Suppression of tumor development and metastasis formation in mice lacking the S100A4(mts1) gene. *Cancer Res* 2005;65:3772–80.
49. Han W, Chen S, Yuan W, Fan Q, Tian J, Wang X, et al. Oriented collagen fibers direct tumor cell intravasation. *Proc Natl Acad Sci USA* 2016;113:11208–13.
50. Burke K, Smid M, Dawes RP, Timmermans MA, Salzman P, van Deurzen CH, et al. Using second harmonic generation to predict patient outcome in solid tumors. *BMC Cancer* 2015;15:929.
51. Kakkad SM, Solaiyappan M, Argani P, Sukumar S, Jacobs LK, Leibfritz D, et al. Collagen I fiber density increases in lymph node positive breast cancers: pilot study. *J Biomed Opt* 2012;17:116017.
52. Maller O, Hansen KC, Lyons TR, Acerbi I, Weaver VM, Prekeris R, et al. Collagen architecture in pregnancy-induced protection from breast cancer. *J Cell Sci* 2013;126:4108–10.
53. Nadiarynkh O, LaComb RB, Brewer MA, Campagnola PJ. Alterations of the extracellular matrix in ovarian cancer studied by second harmonic generation imaging microscopy. *BMC Cancer* 2010;10:94.
54. Rubbens MP, Driessen-Mol A, Boerboom RA, Koppert MM, van Assen HC, TerHaar Romeny BM, et al. Quantification of the temporal evolution of collagen orientation in mechanically conditioned engineered cardiovascular tissues. *Ann Biomed Eng* 2009;37:1263–72.

# Cancer Epidemiology, Biomarkers & Prevention

## Collagen Alignment as a Predictor of Recurrence after Ductal Carcinoma *In Situ*

Matthew W. Conklin, Ronald E. Gangnon, Brian L. Sprague, et al.

*Cancer Epidemiol Biomarkers Prev* 2018;27:138-145. Published OnlineFirst November 15, 2017.

**Updated version** Access the most recent version of this article at:  
doi:[10.1158/1055-9965.EPI-17-0720](https://doi.org/10.1158/1055-9965.EPI-17-0720)

**Supplementary  
Material** Access the most recent supplemental material at:  
<http://cebp.aacrjournals.org/content/suppl/2017/11/14/1055-9965.EPI-17-0720.DC1>

**Cited articles** This article cites 48 articles, 9 of which you can access for free at:  
<http://cebp.aacrjournals.org/content/27/2/138.full#ref-list-1>

**Citing articles** This article has been cited by 3 HighWire-hosted articles. Access the articles at:  
<http://cebp.aacrjournals.org/content/27/2/138.full#related-urls>

**E-mail alerts** [Sign up to receive free email-alerts](#) related to this article or journal.

**Reprints and  
Subscriptions** To order reprints of this article or to subscribe to the journal, contact the AACR Publications Department  
at [pubs@aacr.org](mailto:pubs@aacr.org).

**Permissions** To request permission to re-use all or part of this article, use this link  
<http://cebp.aacrjournals.org/content/27/2/138>.  
Click on "Request Permissions" which will take you to the Copyright Clearance Center's (CCC)  
Rightslink site.